

# VLA HI imaging of the brightest spiral galaxies in Coma

H. Bravo-Alfaro

*Observatoire de Paris DAEC, and UMR 8631, associé au CNRS et à l'Université Paris 7, 92195 Meudon Cedex, France.*

*Departamento de Astronomía, Universidad de Guanajuato. Apdo. Postal 144 Guanajuato 36000. México.*

V. Cayatte

*Observatoire de Paris DAEC, and UMR 8631, associé au CNRS et à l'Université Paris 7, 92195 Meudon Cedex, France.*

J. H. van Gorkom

*Department of Astronomy, Columbia University, New York, New York 10027.*

and

C. Balkowski

*Observatoire de Paris DAEC, and UMR 8631, associé au CNRS et à l'Université Paris 7, 92195 Meudon Cedex, France.*

## ABSTRACT

We have obtained 21 cm images of 19 spiral galaxies in the Coma cluster, using the VLA in its C and D configurations. The sample selection was based on morphology, brightness, and optical diameters of galaxies within one Abell radius ( $1.2^\circ$ ). The HI detected, yet deficient galaxies show a strong correlation in their HI properties with projected distance from the cluster center. The most strongly HI deficient ( $\text{Def}_{\text{HI}} > 0.4$ ) galaxies are located inside a radius of  $30'$  ( $\sim 0.6$  Mpc) from the center of

Coma, roughly the extent of the central X-ray emission. These central galaxies show clear asymmetries in their HI distribution and/or shifts between the optical and 21 cm positions. Another 12 spirals were not detected in HI with typical HI mass upper limits of  $10^8 M_{\odot}$ . Seven out of the twelve non detections are located in the central region of Coma, roughly within  $30'$  from the center. The other non detections are to the east and southwest of the center.

Seven so called blue disk galaxies in Coma were observed in HI and six were detected. These galaxies are relatively close to the central region of Coma. The non detected one is the closest to the center. The six detected blue galaxies are mildly HI deficient. We did a more sensitive search for HI from 11 of the 15 known post starburst galaxies in Coma. None were detected with typical HI mass limits between 3 and  $7 \times 10^7 M_{\odot}$ .

Our results present and enhance a picture already familiar for well studied clusters. HI poor galaxies (deficient ones and non-detections) are concentrated toward the center of the cluster. The HI morphology of the central galaxies, with optical disks extending beyond the HI disks is unique to cluster environments and strongly suggests an interaction with the IGM. A new result in Coma is the clumpy distribution of gas deficiency. In the cluster center the deficient galaxies are to the east while the non-detections are to the west. In the outer parts the gas rich galaxies are north of Coma, non-detected spirals are found in the NGC 4944 group to the east and NGC 4839 group to the south west. This supports recent findings that merging of groups is ongoing in the center of Coma, further out the NGC 4944 and NGC 4839 must have passed at least once through the core, while the galaxies to the north have yet to fall in.

*Subject headings:* Galaxies: Clusters: Individual: Coma

## 1. Introduction.

Two of the outstanding questions on cluster of galaxies are: what causes the density morphology relation and how dynamically relaxed are clusters. For the density morphology relation the question is: are all galaxies formed by the same process and do they evolve differently in different environments? Or does the environment play a dominant role at the time of formation? On a larger scale the question is whether clusters at low redshift are dynamically relaxed or whether they are still accreting significant amounts of mass. The answer to this question may contain a clue to the density of the universe (Thomas et al. 1998). Observations of clusters at intermediate redshift suggest that clusters evolve rapidly. Already at intermediate redshifts they differ markedly from clusters at low redshifts. Many clusters at redshifts larger than  $z \sim 0.3$  are known to contain a large population of blue galaxies, indicative of enhanced star formation, which is not found in similar clusters at  $z < 0.1$  (Butcher & Oemler 1978, 1984; Dressler & Gunn 1992, Poggianti et al. 1999, Dressler et al. 1999). Secondly these clusters often contain galaxies which have recently undergone a starburst, but which are not currently forming stars, displaying spectra with strong Balmer absorption lines but no emission lines at all. These galaxies are commonly referred to as “post-starburst” (PSB) galaxies.

We address both questions with HI imaging studies of nearby clusters, which are directly comparable to more distant ones. Detailed HI imaging of the nearest cluster of galaxies, Virgo, has shown that the neutral gas component gets affected dramatically by the hot intergalactic medium (IGM) (van Gorkom et al. 1984, Warmels 1988, and Cayatte et

al. 1990, 1994). In the center of Virgo the HI disks are much smaller than the optical disks. The actual HI removal mechanisms at work in the center of Virgo could be identified by a detailed comparison of the HI surface density distribution of the cluster galaxies with their counterparts in the field (Cayatte et al. 1994). Thus, the HI distribution of individual galaxies reflects the effect of the cluster environment, while the location and velocities of gas-rich versus gas-poor galaxies can help identify possible substructure in the clusters (Valluri et al. 1999). Gas can also be used to probe the orbital history of the galaxies. More recently other clusters have been imaged in HI with the VLA and WSRT: Hydra (McMahon 1993), Ursa Majoris (Verheijen 1996), A 2670 (van Gorkom 1996), A 262 (Bravo-Alfaro et al. 1997), and Hercules (Dickey 1997). Preliminary results on Coma were obtained by Sullivan (1989) in the early days of the VLA. In spite of poor sensitivity and interference problems in the data, he observed disturbed HI disks for a few galaxies in the center.

In this paper we present a more complete and much more sensitive study of the Coma cluster. We expect the environmental effects in Coma to be stronger than in Virgo, because Coma is a much richer cluster and because its central X-ray emission is almost six times more luminous than in Virgo. Indeed, single dish observations have shown that Coma is one of the most HI deficient clusters; extremely HI deficient galaxies are seen out to  $1.5 r_A$  (the Abell radius,  $r_A = 1.7'/z$ , where  $z$  is the redshift), while in other clusters strongly HI deficient galaxies are generally not seen beyond  $0.75 r_A$  (Bothun et al. 1985; Giovanelli and Haynes 1985; Gavazzi 1987; 1989). The Coma cluster is in fact the

richest of the nearby clusters (richness class 2, and  $z = 0.023^1$ ), and represents the closest equivalent to what is seen at intermediate redshifts, as it has blue disk galaxies (Bothun & Dressler 1986, and references therein) and PSB galaxies (Caldwell, Rose, & Dendy 1999, and references therein), which are commonly seen in distant clusters. This makes Coma the perfect link between nearby and more distant clusters.

In the present paper we discuss the global properties of Coma, on the basis of our HI results, combined with recent observations on different wavelengths and numerical work. A detailed analysis of individual galaxies and more specific regions of Coma, will be the subject of a forthcoming paper (Bravo-Alfaro et al. 1999). The plan of this paper is as follows: Observations and data reduction are described in Section 2. Observational results are given in Section 3. In Section 4 we discuss what the observations have taught us about Coma at large. Conclusions are summarized in Section 5. A description of HI properties of individual galaxies is given in Appendix A.

## 2. Observations

We selected the 25 brightest spiral galaxies in Coma with morphological type later than S0. All those galaxies have B magnitude smaller than 15.7 mag and optical diameters larger than  $0.5'$ . Fig. 1 shows the location of the 12 fields observed with the VLA,<sup>2</sup> up to  $1.2^\circ$  ( $1 r_A$ ) from the center of Coma (we take the position of NGC 4874 as the Coma cen-

ter). Three fields (1, 2, and 9) are centered around the core, covering most of the Coma velocity range. Field 8 was pointed south of the elliptical NGC 4839, which is the dominant galaxy of the SW group. Five other fields (3, 4, 6, 7, and 10) contain the blue disk galaxies reported by Bothun & Dressler (1986) and most of the PSBs reported by Caldwell et al. (1993) and Caldwell & Rose (1997). The remaining three fields (5, 11, and 12) were centered in the outer regions of the cluster, where no strong environmental effects are expected, providing a comparison sample.

The VLA survey of Coma was carried out in C and D array, during three runs, in March 1995, April 1996, and March 1999. In March 1995, an exploratory observation was done of fields 2, 4 and 5, in D array. Twelve fields were observed in C array in April 1996. Fields 1 and 10 were reobserved, March 1999, to get very sensitive observations of the PSB galaxies in these fields. For the fields observed in both, C and D configurations (fields 1, 2, 4, 5, and 10), the data were combined to improve sensitivity. The combined data provide the higher spatial resolution and a lower velocity resolution. In the D array observations of 1995 online Hanning smoothing was used, after which every other channel was discarded. This leaves a set of 31 independent channels with a velocity spacing of 43 km/s. In C array no online Hanning smoothing was used, providing a set of 63 channels with a velocity resolution of 21.7 km/s. Most of these observations were afterwards Hanning smoothed to the same velocity resolution as the D array data. The C array data were tapered to an angular resolution of 30 arcsec, and, in most cases, we obtained a resolution of 35 arcsec for the combined C+D data.

Standard VLA calibration and imaging pro-

<sup>1</sup>We assume a velocity of  $7000 \text{ km s}^{-1}$ , and  $H_0 = 100 \text{ km s}^{-1} \text{ Mpc}^{-1}$  throughout this paper.

<sup>2</sup>The National Radio Astronomy Observatory is operated by Associated Universities, Inc., under cooperative agreement with the National Science Foundation.

cedures were applied, using the NRAO’s astronomical image processing system (AIPS). Data cubes were made using nearly pure natural weighting to obtain a higher sensitivity. A set of eight line-free channels on either side of the band was used (four channels in the case of C+D combined data) to define a mean continuum image. This image was then subtracted from the channel maps forming an HI line emission cube. We used this cube to search for 21 cm line emission and to determine the spatial position and velocity range for each signal. Finally, a new continuum image was made using only line-free channels. The channels containing line emission were CLEANed (for more details on data reduction see Bravo–Alfaro 1997). The rms in the final cubes is typically 0.37 mJy/beam per channel. The observations have on average an HI mass detection threshold of  $10^8 M_{\odot}$ , corresponding to  $6 \times \sigma \times 21.7 \text{ km sec}^{-1}$  (the channel width) and a typical surface brightness sensitivity of 2 to  $4 \times 10^{19} \text{ cm}^{-2}$  (corresponding to 2.5 rms). Fields 1 and 10, were reobserved in 1999 for 20 and 15 hours respectively; there our detection thresholds are lower: the rms per channel is around 0.20 mJy/beam, and the HI mass detection threshold is  $2.4 \times 10^7 M_{\odot}$  in the center of the field.

The observational parameters are listed in Table 1, where Column 1 indicates the observed field, Columns 2 and 3 give R.A. and Dec. (1950) of each pointing, Column 4 gives the VLA configuration, Column 5 the integration time, Column 6 the total bandwidth, Column 7 the heliocentric velocity of the central channel, Column 8 the channel separation (in  $\text{km s}^{-1}$ ), Column 9 the rms noise per channel after the continuum subtraction, and Column 10 the flux density per beam area (in mJy/beam) equivalent to 1.0 K in the channel

maps.

### 3. Results

We detected 19 galaxies in this survey; 17 spirals, one irregular, and one interacting system. Table 2 lists those galaxies with their observational parameters. Columns 1 and 2 give the galaxy identification, Column 3 and 4 the R.A. and Dec. (1950) from the NED data base, except (1) taken from the LEDA data base, Column 5 gives the VLA configuration, Column 6 the synthesized beam size (in arcsec), Column 7 gives the morphological type from Dressler 1980, except when indicated: (1) from Huchra et al. 1990, (2) from the LEDA database, and (\*) for uncertain classification. Column 8 gives the blue total magnitude obtained from the LEDA database, except (1) taken from the NED database; Column 9 gives the  $m_{UV-b}$  color, from Donas et al. 1995.

In Table 3 we list the HI parameters derived from the observations: Columns 1 and 2 are as in Table 2, Column 3 gives the observed field, Column 4 and Column 5 give the central HI velocity and the velocity width, respectively. As the signal-to-noise ratio is poor for some galaxies, we use as a homogeneous criterium to obtain the central HI velocity the central channel displaying emission. The uncertainty in this value is around half the velocity resolution, i.e.  $\sim 11 \text{ km s}^{-1}$ . The velocity width is defined as given by the range of channels containing HI emission. The error in this case is the velocity resolution, around  $22 \text{ km s}^{-1}$ . Column 6 gives the HI total flux corrected for the primary beam attenuation, with the corresponding error. Column 7 gives the continuum intensity, Column 8 the total HI mass, Column 9 and 10 give the HI deficiency and the projected distance from the

cluster center respectively.

The main result of this paper is summarized in Fig. 2. It shows a synthetic view of all the galaxies detected in HI. They are placed at their correct location in the cluster and magnified by a factor 7. Contours of the individual HI images (the first contour corresponds to a column density of  $3 \times 10^{19} \text{ cm}^{-2}$ ) are overlaid on optical images shown in grey-scale (DSS). The cross indicates the center of the cluster (taken to be the position of NGC 4874), and the central contours draw the X-ray emission in the 0.5–2 keV energy band, as observed with ROSAT (Vikhlinin, et al. 1997). This figure displays a wealth of information. As in Virgo, the first thing to note is that the HI disks in the outer parts of the cluster are much larger than the optical disks. But something different in Coma, are the asymmetries and even displacements of the shrunken HI disks seen in the center. All the shrunken HI disks are in projection within the boundaries of the X-ray emission (see Fig. 2), suggesting that an interaction with the IGM may be at work. Near the cluster center, the distribution of HI detected galaxies is very non uniform: most of the detections lie east of the center, and there are almost no detections west of the center. In the zone between the center of Coma and the SW group, only one galaxy (Mrk 058), with very low gas content, was detected.

Twelve galaxies from the original observed sample (morphological type later than S0 and  $m_B < 15.7$ ) were not detected (Table 4). They are within  $20'$  from the center of the observed fields and within the observed velocity range. Table 4 gives in Columns 1 and 2 the identification, Columns 3 and 4 the R.A. and Dec. (1950), in Column 5 the observed field, Column 6 gives the morphologi-

cal type taken from Dressler 1980, except (1) taken from Huchra et al. 1990, (2) from the NED database, and (3) from the RC3 catalog; (\*) means uncertain classification. Column 7 gives the optical velocity taken from the LEDA database, Column 8 the rms noise per channel corrected for the primary beam response at the position of the galaxy. The HI mass upper limit given in Column 9 corresponds to 6 times the rms noise, multiplied by the channel width (typically  $21.7 \text{ km s}^{-1}$ ). Column 10 gives the lower limit to the HI deficiency.

In addition, we made a special effort to detect the so called abnormal spectrum galaxies, reported in Coma by Caldwell et al. (1993) and Caldwell and Rose (1997). Some of them display ongoing star formation activity (SB), and others a recent peak of star formation (PSB). Most of these galaxies are found southwest of the cluster center (see Sect. 3.4.2). In Table 5 we give a list of all the peculiar spectrum galaxies observed in this survey; none was detected in HI. Column 1 and 2 give the galaxy identification (the first corresponds to the Dressler, 1980 catalog number), Column 3 gives the observed field, Column 4 and 5 the (1950) R.A. and Dec. Column 6 the morphological type, and Column 7 the heliocentric velocity, both from the NED database. Column 8 gives the rms noise per channel corrected for the primary beam response at the position of the galaxy. Column 9 gives the HI mass upper limit for both, SB and PSB non detected galaxies, typically between 3 and  $7 \times 10^7 M_{\odot}$ . We did not estimate the HI deficiency parameter, as most of these galaxies are lenticular (morphological type S0).

### 3.1. The HI Content

### 3.1.1. Comparison with previous works

Five of the 19 detected galaxies are new HI detections. Three of them (FOCA 195, KUG 1255+275, and KUG 1258+287) are HI rich systems with relatively low optical surface brightness, which have not been observed previously in single dish HI surveys. NGC 4907 and CGCG 160–106, were not detected in previous single-dish HI surveys probably because of their low total HI flux (see Table 3). CGCG 160–106 was already detected with the VLA by Sullivan (1981). Four of the galaxies detected in the present survey (NGC 4907, CGCG 160–106, Mrk 058, and IC 4040), were not detected in the most recent survey carried out with the Arecibo telescope (Haynes et al. 1997), either because of low HI flux, or because several objects were found inside the beam.

In Fig. 3 we show a comparison between single dish and VLA measurements. There is in general a good agreement, showing that the VLA has not missed any extended flux. Two discrepant cases are seen in Fig. 3, NGC 4848 and IC 842. We obtained for the former, systematically a lower total HI flux than the values previously reported (Chincarini et al. 1983, Giovanelli & Haynes 1985, Gavazzi 1989 and Haynes et al. 1997). We confirm the asymmetric distribution found by Gavazzi (1989) but we probably miss some extended HI emission. We obtained for IC 842 a slightly higher HI flux ( $\sim 30\%$ ) than previous single dish observations (Chincarini et al. 1983, Bothun et al. 1985, Gavazzi 1989, and Haynes et al. 1997).

We do not confirm two detections previously reported, Mrk 056 and NGC 4944, which were only marginally detected by Gavazzi (1987). Our HI flux upper limit for Mrk 056 (CGCG 160–064) is well below the flux mea-

sured by Gavazzi. This galaxy is very close to the detected HI rich galaxy KUG 1255+275, both spatially ( $4.6'$ ) and in velocity, thus this result may be due to confusion inside the Arecibo beam. On the other hand, the detection of NGC 4944 is reported by Gavazzi (1987) as a marginal one, and it was not confirmed in later surveys (e.g. Gavazzi 1989).

### 3.1.2. The HI deficiency

To quantify the HI content of the spirals as compared to so called field spirals we use the HI deficiency parameter ( $\text{Def}_{\text{HI}}$ ), following the definition by Giovanelli & Haynes (1985, and references therein), where the deficiency parameter is the log of the ratio of the average HI mass of isolated spirals of the same morphological type and the observed HI mass. For our sample, we use the morphological types from Dressler (1980), or from Huchra et al. (1990) when the first is not available. We should remark that the HI deficiencies in Coma are less well defined than for more nearby clusters due to considerable uncertainty in the morphological classification.

A diagram of the HI deficiency versus projected distance to the cluster center is shown in Fig. 4, where all detected galaxies are shown with black circles and lower limits for non detections (only galaxies from Table 4 are included in this figure) with triangles. The merging system NGC 4922 is not plotted in this figure because of its peculiarity (see Appendix A). Clearly the most HI deficient galaxies are closer to the cluster core. All strongly HI deficient detected galaxies ( $\text{Def} > 0.4$ ) are inside a projected radius of  $30'$  ( $0.4r_A$ ) from the center of Coma. For the non detected galaxies the trend of deficiency with the projected distance to the center is not as clear as it is for the detected ones, but

7 of the non-detections are projected inside or very close to the X-ray emission (UGC 8071, NGC 4851, IC 3943, NGC 4858, IC 3955, KUG 1258+277, and CGCG 160-261), as shown in Fig. 5.

For the non detected galaxies we used 6 times the r.m.s. multiplied by the velocity channel width to calculate both, the deficiency and the HI mass upper limit shown in Table 4. This value is estimated on the basis of our detection threshold. Another method to estimate the HI mass upper limit for non detected galaxies could consider the expected velocity width for a big spiral, e.g.  $300 \text{ km s}^{-1}$ , rather than the observed channel width. In this fashion the total flux upper limit would be obtained as  $\text{r.m.s.} \times 2.5 \times 300 \text{ km s}^{-1}$ . But as these galaxies are not in a typical environment we do not know at all what the HI velocity width could be after a stripping process. Using this different limit does not substantially change the plot in Fig. 4.

Although a possible correlation with distance to cluster center can be considerably weakened by projection effects (Chamaraux et al. 1980), the fact that the most deficient galaxies are almost all situated within the central and southwestern X-ray emission suggests that an interaction with the IGM is at work. More convincing evidence for this can be obtained by looking at the relative sizes of the HI disks. No other mechanism would cause the HI disks to be smaller than the optical ones. We will address these issues in a following paper.

### 3.2. The central region

Fig. 5 shows the position of the detections with crosses, and the 12 non detected galaxies with triangles. We consider here as non detections those galaxies brighter than a mag-

nitude of 15.7, with morphological type later than S0 (Table 4). We also show in Fig. 5 the contours of the X-ray emission (ROSAT) centered on Coma, as reported by Vikhlinin et al. (1997). The central region of Coma contains most of the strongly HI deficient galaxies in the cluster, including the very bright early spirals NGC 4911, NGC 4921, and NGC 4907, all of them very HI deficient. The giant spiral NGC 4911, detected in X-ray, is thought to be the dominant galaxy of a group crossing the main Coma body. NGC 4921 (classified as “anemic” by van den Bergh, 1976) and NGC 4907 show very perturbed HI maps; they have large velocities relative to the mean cluster velocity ( $1179$  and  $1521 \text{ km s}^{-1}$  respectively). Four other galaxies were detected inside a radius of  $30'$  ( $\sim 0.60 \text{ Mpc}$ ) which is roughly the area defined by the X-ray emission shown in Fig. 5. With no exception these galaxies show deeply perturbed HI distributions, some of them smaller than the corresponding optical disks (see Fig. 2).

### 3.3. The SW of Coma

The presence of a group in the SW of Coma, associated with the giant elliptical galaxy NGC 4839, has been well established through optical and X-ray studies (e.g. Briel et al. 1992, White et al. 1993, Colles & Dunn 1996, Biviano et al. 1996). The group sits  $40'$  SW of the cluster core, and coincides with the second most intense X-ray peak. This group represents 6% of the total X-ray emission, and contains about 10% of the mass of the cluster. The question whether this group is falling into the center of Coma (Colles & Dunn 1996), or has already passed following a straight path (Burns et al. 1994), is still a matter of debate. Recently, Caldwell & Rose (1997) concluded that the SW group



has already passed through the main body of Coma, based on the velocity structure of the group and the presence of PSB galaxies in that zone. Our field number 8, which includes NGC 4839, and field number 10 in the zone between this galaxy and the cluster center, try to clarify this controversy.

Of the 18 galaxies surrounding NGC 4839 and belonging to the group (Biviano 1998), four were observed and none were detected. This is perhaps not too surprising since all of them are classified as S0. We did however detect three late type galaxies just south of the NGC 4839 group (IC 3913, KUG 1255+275 and Mrk 057), just outside the X-ray emission (Figs. A2 and A5). Their radial velocities are close to the systemic velocity of the group ( $7339 \pm 329 \text{ km s}^{-1}$ , Colless & Dunn 1996), thus they are likely to be group members. These galaxies have undisturbed morphologies and a normal HI content, which makes it extremely unlikely that they have crossed the cluster core.

Our HI results are inconclusive. The non detections in the close vicinity of NGC 4839, and the presence of several SB and PSB galaxies in that zone with a very low HI content (see Sect. 3.4.2 and Table 5), support the hypothesis that the group has gone through. The 3 gas rich galaxies pose a problem. If they are members of the group, the group cannot have passed through the main cluster. Alternatively they may be new members of the group, only recently accreted after the group has gone through the cluster center.

### 3.4. HI content of SB and PSB galaxies in Coma.

#### 3.4.1. The blue disk galaxies

As mentioned before Coma contains blue disk and post-starburst galaxies, similar to those seen at intermediate redshifts. Bothun & Dressler (1986) obtained spectroscopy for seven blue galaxies in Coma, and showed that they had not only experienced a star burst, but were still forming stars at a high rate. Considering various mechanisms to produce the starburst phenomena these authors conclude with a mild preference for ram pressure induced star formation. The main reason for rejecting galaxy-galaxy induced star formation is that the blue disks do not appear to be interacting (except the non detected NGC 4858, possibly interacting with NGC 4860 and member of an *aggregate*, Conselice and Gallagher 1998). All seven blue disk galaxies were observed in this survey and six of them were detected: NGC 4848, Mrk 058, CGCG 160-086, IC 4040, CGCG 160-098 and NGC 4926-A. The first four are projected inside the X-ray emission (Fig. 6) and are HI deficient ( $\text{Def}_{\text{HI}} > 0.5$ ). They display very perturbed HI distributions. The HI deficiencies and gas distribution strongly suggest that these galaxies are being ram pressure swept by the IGM.

The locations of the HI detected blue disk galaxies are indicated with crosses in Fig. 6. Most of them are in an annular region between 20' and 30' from the cluster center, which coincides with the outermost contour of the X-ray emission (corresponding to a gas density of  $\sim 3 \times 10^{-4} \text{ cm}^{-3}$ ). This is similar to what has been seen in Butcher-Oemler clusters, where blue galaxies seem preferentially located in an annular region outside the cluster core (e.g. Butcher and Oemler 1984; Mellier et al. 1988). Dressler & Gunn (1990) reported that star forming galaxies

seem to avoid the cluster core, appearing first at a radius of  $\sim 0.5$  Mpc ( $0.5$  Mpc= $25'$  in Coma). Furthermore, the UV survey of Coma by Donas et al. (1995) revealed that 38% of the UV flux is produced in a ring lying between  $20'$  and  $30'$  of the cluster center. This suggests that this effect must be related to the global properties of the cluster, perhaps IGM induced star formation can best explain the shell of blue starburst seen in Coma and similarly in high redshift clusters (Oemler 1992).

We also show in Fig. 6, with triangles, the non-detected blue disk galaxy (NGC 4858) and three starburst like objects reported by Caldwell et al. (1993), which were also not detected in this survey (Table 5). The blue disk is projected well inside the X-ray emission and star formation followed by ram pressure stripping may have exhausted their HI reservoir. The other three galaxies show abnormal spectra with strong emission lines (Caldwell et al. 1993). These objects are also near the edge of X-ray emission, in the SW direction. Their non detection suggests that in this zone, between the center and the SW group, the gas is more easily removed. Note that starbursting galaxies in other directions (e.g. NGC 4848, IC 4040, and CGCG 160-086), at similar distances from the center, are detected in HI.

### 3.4.2. *The post starburst galaxies*

Caldwell et al. (1993) and Caldwell & Rose (1997) reported a total of 22 abnormal spectrum galaxies in Coma. Five of them display Balmer absorption and emission lines (see previous paragraph), two AGN's, and 15 galaxies show enhanced Balmer absorption lines but no emission, similar to PSBs observed in  $z\sim 0.3$  clusters. Most of the PSBs in Coma are early type objects (mostly S0's).

The spectra indicate that a burst of star formation was recently truncated ( $\sim 1$  Gyr ago). Among the 15 PSBs 8 are in the SW region, the remaining are near the center and in the NE (Caldwell et al., 1993). We observed 11 of those galaxies, and detected none (see Table 5). The position of those galaxies are shown in Fig. 6 with dotted circles. The X-ray contours (Vikhlinin et al. 1997) are also drawn.

The NGC 4839 group has an average velocity close to the peak in the PSBs velocity distribution (Biviano et al. 1996). This suggests that the PSBs could be part of the group and they have been stripped of their gas when they passed through the Coma core. The few PSBs in the center and NE of Coma could be old members of the SW group, previously pulled out from the group when it passed through the cluster center (Caldwell et al. 1993).

Our results suggest an evolutionary sequence, where galaxies first become blue because of IGM induced star formation. Star formation and further ram pressure stripping makes them HI deficient. The displaced and shrunken HI disks of the blue disk galaxies indicate that some interaction with the IGM is indeed going on. The next step in this evolutionary sequence is the PSB phase, where galaxies have lost most of the HI gas, and as consequence, star formation stops on a relatively short time scale. In this picture all the PSBs would be in an advanced stage of gas stripping.

### 3.4.3. *Correlation between Colors and HI-Deficiency*

Although gas is needed for star formation it is not obvious that only the atomic gas content is related to star formation ac-

tivity (Donas et al. 1990). Molecular clouds are denser and more centrally located in the galaxies, making it less likely that this component will be affected by the cluster environment. For example Kenney & Young 1989 (and references therein) showed in Virgo, and Casoli et al. (1991) in the Coma supercluster, that there is no evidence for a lower molecular content than in the field, even for the HI deficient galaxies. For instance, the starburst NGC 4858, which is not detected in HI in the present survey ( $\text{Def}_{\text{HI}} > 0.93$ ), shows normal CO emission. The same is true for the detected, yet HI deficient galaxies such as NGC 4848, NGC 4911, and NGC 4921. On the basis of new CO data for galaxies in Coma, Boselli et al. 1997 conclude that no correlation is observed between  $\text{H}_2$  content and the HI deficiency parameter, and that molecular gas is not perturbed by the interaction with the IGM. More recent CO observations for galaxies in Coma, by Lavezzi et al. (1999), give additional support to that conclusion.

While CO and HI do not correlate, we show in Fig. 7 that in Coma star formation does appear to correlate with HI deficiency. In that figure we display the HI deficiency versus the mUV–b color, a very good tracer of star formation. Sixteen of the 19 galaxies in our sample have been observed by Donas et al. (1995) with the imaging UV telescope FOCA (see mUV–b values in column 9 of Table 2). A clear correlation appears in this plot, where the linear fit is shown (the correlation coefficient is 0.61). Points in the bottom right corner of Fig. 7 correspond to the three central early spirals (NGC 4907, NGC 4911, and NGC 4921). This trend, where galaxies with red mUV–b colors are the most HI deficient, has also been found in Virgo by Giovanelli and

Haynes (1983). Thus apparently colors become redder if the interaction with the IGM is effectively stripping the HI gas. As a comparison, we show in Fig. 8 a plot mUV–b vs. the  $M_{\text{H}_2}$  surface density (drawn by the ratio between  $M_{\text{H}_2}$  and the optical disk area) for seven of the most HI deficient galaxies in Coma. This figure shows a weak correlation between the mUV–b color and the molecular content, a high dispersion is seen (the correlation coefficient is only 0.47).

It is worth mentioning that the clear correlation shown in Fig. 7 is not due to a color–morphology trend, as HI deficiency occurs both in early and late spirals. We tested for a possible correlation between the HI deficiency and the morphological type, and the result is that no trend is found (see Column 7 in Table 2 and Column 9 in Table 3). These results suggest that in Coma as in Virgo (Giovanelli and Haynes 1983) stripping has affected the star formation history of the galaxies.

### 3.5. The periphery of Coma; the East and Northern regions.

Three fields were observed in the Coma periphery. The eastern field (Field 11) was centered on the early type spiral NGC 4944, for which we do not confirm Gavazzi’s (1987) detection. Quite surprisingly two other non detections are in this region. Biviano et al. (1996) propose that NGC 4944 is the center of one of the groups in the Coma structure. The general HI deficiency of this group suggests that it already passed through the cluster center.

In the northern region, the HI data confirm the presence of two other groups. The first of them, observed in Field 6, is possibly associated with the blue disk galaxy CGCG 160–098. We detected 3 HI rich galax-

ies in that zone (CGCG 160–098, FOCA 195, and KUG 1258+287). They are separated from each other by distances around 13' ( $\sim 260$  kpc), and their velocities range from  $8426 \text{ km s}^{-1}$  to  $8884 \text{ km s}^{-1}$ . Ours is the first redshift determination of FOCA 195. We also see HI emission, still to be confirmed, 1.4' W of KUG 1258+287, which does not seem to have an optical counterpart on the DSS. The total HI mass is  $2.2 \times 10^8 M_{\odot}$ , a typical value for a dwarf galaxy.

The last field (Field 5) was pointed  $\sim 1.2^{\circ}$  NE of the Coma center. In this field we detected two HI rich galaxies, IC 842, and IC 4088, and the interacting system NGC 4922, located 84' away from the cluster center. The pair NGC 4922 is the brightest IR object in Coma (Mirabel & Sanders 1988), composed of a brighter spiral component in the north, and a fainter lenticular in the south. In addition, the spiral has a central radio continuum source, 5C4.130, with a flux of 60 mJy (Wilson 1970). We detect weak HI emission and confirm the strong absorption feature reported by Gavazzi (1987). We confirm that the HI absorption and emission features are centered on the northern spiral component.

Three HI rich dwarf systems were detected in field 5, associated with the spiral IC 4088. Their HI maps look quite regular. The dwarf galaxies are previously uncatalogued in HI, except [GMP83] 1866, which was reported by Sullivan (1989). This object shows a total HI mass of  $\sim 2.1 \times 10^9 M_{\odot}$ , and a velocity width of  $173 \text{ km s}^{-1}$ . The two other dwarfs have HI masses in the range  $2.2\text{--}6.1 \times 10^8 M_{\odot}$ , and velocity widths of  $43 \text{ km s}^{-1}$  and  $130 \text{ km s}^{-1}$ . The position of these galaxies and the absence of HI rich dwarfs close to the center of Coma, suggests that these systems tend to be present only in the outskirts of the cluster, associated with luminous galaxies. This is supported by

the fact that we devoted only two fields to observe regions far from the X-ray source of Coma, and it is there where HI rich dwarfs appear, while in the remaining more central ten fields (a 5 times larger observed volume), we detected none of these objects.

#### 4. Discussion

The goal of our HI imaging studies of clusters of galaxies is twofold: to investigate the interaction between individual galaxies and the cluster environment and to probe the dynamical state of the cluster. Physical mechanisms affecting individual galaxies will be discussed in a second paper (Bravo-Alfaro et al. 1999), here we place the observational results in the larger context of the cluster evolution.

Several recent papers have discussed the dynamical state of Coma based on the optical mass distribution (Girardi et al. 1994, Biviano et al. 1996, Colles and Dunn 1996), the surface brightness distribution of the X-ray emission (Vikhlinin et al. 1997 and references therein) and the temperature structure of the X ray gas (Donnelly et al. 1999 and references therein). The cluster HI distribution shown in Figures 2, 5 and 6, strengthens some of the arguments used by those authors. These figures show gas rich galaxies associated with the CGCG 160–098 and IC 4088 in the north, a lack of HI in the groups associated with NGC 4944 in the east, NGC 4911 in the center and NGC 4839 in the south. The HI deficient galaxies are east of the center, while the non detection are mostly west of the center. This result is consistent with the recent analysis by Donnelly et al. (1999), who find that there is cooler gas just south and south east of the center, while there is a hot spot in the X-ray gas just north of the center. These

authors argue that most likely the NGC 4874 group is a recent arrival in Coma, leaving behind a cool trail of gas, the hot spot would then be the bow shock generated as the group moves through the IGM. Interestingly numerical simulations show (Roettiger et al. 1996) that in minor mergers the infalling object will first develop a protective bow shock, which will shelter the galaxies from being ram pressure stripped. Close to core passage the infalling object's ISM encounters a rapidly increasing density, leading to a burst of ram pressure stripping. This may explain that we do detect galaxies east and south east of the center, though they are HI deficient, while our non detections are mostly west of the center and those galaxies have probably already passed the core. Note that several of the small HI disks in Coma are very asymmetric, indicative of current stripping, since any asymmetry would be smeared out in roughly one rotation period ( $\sim 10^8$  years).

A question that remains is what triggered and stopped the starburst in the blue disk galaxies and PSBs respectively. Several mechanisms have been suggested, galaxy-galaxy interactions (Combes et al. 1988), galaxy harassment (Moore et al. 1996, 1999), potential of a group-cluster interaction (Bekki 1999), and ISM-IGM interactions (Poggianti et al. 1999 and references therein). Least likely of those is the galaxy-galaxy interaction scenario. The blue disks are located close to the center, in the outskirts of the X ray source and show no optical signs of being disturbed. Our HI observations showed that it is the galaxies in the outer parts of the cluster that have gas rich companions, while most of the center galaxies appear more isolated. We investigated this further by counting the number of galaxies inside a 5 arcmin circle around each of the

galaxies in Tables 2 and 3. Five arcmin corresponds to 100 kpc at the distance of Coma, encounters at larger distances are unlikely to be effective (Moore et al. 1999 suggest that an encounter with an impact parameter of 60 kpc is typical in a rich cluster of galaxies). The number of neighbours was taken from NED, which unfortunately has rather incomplete velocity information. In Figure 9 we plot mUV-b color versus number of close neighbours. Clearly no correlation is seen in this plot, and blue galaxies do not show an excess of close neighbours (if the weak trend in the opposite direction was real, it would mean that red objects have a slightly larger number of neighbours).

The location of the blue disk galaxies and the observation that the UV radiation peaks in an annulus 20 arcmin from center (Donas et al. 1995), something which has also been found in more distant clusters (Butcher and Oemler 1984, Mellier et al. 1988, Dressler & Gunn 1990, Dressler et al. 1999), makes it more likely that the starbursts are caused by gas-gas interaction or an interaction with the global cluster potential. The fact that the blue disk galaxies are HI deficient and have lost their gas in the outer parts, makes an ISM-IGM interaction slightly more plausible than the interaction with a tidal field (Bekki 1999). Tidal interactions tend to move gas toward the center and outward (Barnes, 1998), thus even if it is the tidal interaction that causes the burst, the gas in the outer parts must still have been removed some other way. Numerical work by Stevens et al. (1999) shows that interaction between galaxies and the IGM may produce mass loss and features like bow-shocks and stripped tails (observed in X-ray), that should be present in cluster with different degrees of richness. These effects are well

known to prelude star formation activity. Observationally, most of the detected blue disks in the present survey are projected inside or at the edge of the X-ray emission and they seem to have lost their HI in the outer parts, while the non detected blue disk (NGC 4858) sits even deeper within the X-ray source. It is especially the loss of HI in the outer parts of galaxies that is suggestive. Of the PSB galaxies none is detected in HI, and most of them are located within the X-ray source. Thus it seems plausible that in Coma at least the starburst gets triggered by an interaction with the IGM and the starburst is likely to stop because most of the remaining gas gets swept out of the galaxies.

## 5. Summary

We carried out a 21 cm survey of the Coma cluster with the VLA. High resolution images were obtained for 19 spiral galaxies inside  $1r_A$  ( $1.2^\circ$ ). Five of the galaxies in the present survey are new detections in 21 cm.

- We find gas rich and gas poor groups of galaxies in Coma that can be isolated in space and velocity. The groups north of the cluster are gas rich while groups associated with NGC 4944 to the east and NGC 4939 to the southwest are HI poor. Even in the cluster center asymmetries occur, the galaxies west of the center are very HI deficient with small HI disks, while the galaxies east of the center are not detected at all in HI. We suggest that the most HI poor groups have gone through the center, while the deficient galaxies east of the center are currently falling and being stripped.

- As expected, the environmental effects on the HI properties of spirals in Coma are stronger than those previously reported in Virgo, where the IGM is less dense than in Coma.

- We confirm the tendency of HI deficient galaxies to be closer to the cluster core: seven of the detected galaxies are very HI deficient ( $\text{Def}_{\text{HI}} > 0.4$ ), and they lie inside a radius of  $30'$  from the cluster center. This zone roughly coincides with the X-ray emission. With no exception these galaxies show very perturbed HI distributions. For most of them ram pressure by the dense IGM is a likely explanation of their abnormal HI properties, but also other mechanisms, such as viscous stripping and conversion of HI to molecular gas, are probably present.

- Six blue disk galaxies are detected in Coma in HI. Four of them are HI deficient and they are projected inside an annular zone between  $20'$  ( $0.4$  Mpc) and  $30'$  ( $0.6$  Mpc) from the cluster center. This has been observed in high redshift clusters where star forming galaxies seem to avoid the cluster core, appearing first at a radius of  $\sim 0.5$  Mpc. This annulus roughly coincides in Coma with the outer region of the X-ray emission as well as the peak of UV emission. This confirms a close correlation between the location of star forming galaxies and global properties of the cluster.

- Eleven PSBs were observed in this survey but none was detected; HI mass upper limit as low as  $3 \times 10^7 M_\odot$  are found. Most of these galaxies are projected onto the hot IGM medium outlined by the X-ray emission.

- We find a correlation between HI deficiency and UV-b color, in the sense that the most deficient galaxies are reddest. This suggests that the loss of atomic gas reduces the star formation rate, despite the fact that the molecular gas seems hardly affected.

We thank the NRAO for generous allocation of observing time and the VLA staff

for help with the observations. HBA thanks the CONACYT of Mexico, for its support through a Ph.D. grant, and the Mexico–USA Foundation for Science, for its support through a summer grant. HBA also thanks the DAEC of the *Observatoire de Paris*, the Astronomy Department of Columbia University, and the AOC of the NRAO, for its support and hospitality during his visits. JHvG was supported by an NSF grant to Columbia University. JHvG and HBA thank the organizers of the 1998 Guillermo Haro Workshop on the Formation and Evolution of Galaxies at INAOE, where part of this work was done. We have made use of the Lyon-Meudon Extragalactic Database (LEDa) supplied by the LEDa team at the CRAL-Observatoire de Lyon (France). We used NED, the NASA/IPAC extragalactic database, operated for NASA by the Jet Propulsion Laboratory at Caltech. We used the Digital Sky Survey, produced at the Space Telescope Science Institute.

#### A. Description of HI properties

- **IC 3913** This late type spiral is one of the three galaxies detected in the SW of Coma, lying at  $17'$  (0.34 Mpc) SW of NGC 4839. IC 3913 shows a normal HI content ( $\text{Def}_{\text{HI}}=0.04$ ) and a regular HI distribution). Its most external HI contour displays a clear extension to the east, what accounts for the asymmetry observed by Gavazzi (1989) from single dish observations.
- **NGC 4848** This blue disk Scd galaxy, projected on the NE edge of the X-ray source, shows one of the most perturbed gas distribution of this survey, and a high HI deficiency ( $\text{Def}_{\text{HI}}=1.14$ ). However, this value should be taken with care, as Fig. 3 shows that our HI flux value is systematically lower than in previous single dish surveys, what suggests we lost some flux in the central region. Nevertheless, the asymmetric HI distribution most be real, with most of the neutral hydrogen in the north as reported by Gavazzi (1989).
- **CGCG 160–058** This late type spiral galaxy, in the NE of Coma, shows an HI distribution extending slightly further than the optical disk. We obtained a normal HI content ( $\text{Def}_{\text{HI}}=0.12$ ), contrary to Sullivan (1989), who obtained a smaller HI extent than the optical disk and a slight HI deficiency ( $\text{Def}_{\text{HI}}=0.4$ ).
- **KUG 1255+275** This irregular galaxy, in the SW of Coma, is detected for the first time in 21 cm. It is an HI rich galaxy ( $\text{Def}_{\text{HI}}=-0.17$ ), with rather regular gas distribution.
- **Mrk 057** This galaxy is located SE

from NGC 4839. It is a very HI rich galaxy ( $\text{Def}_{\text{HI}}=-0.44$ ), with an HI distribution displaying an extension to the north.

- **Mrk 058** This blue disk galaxy, in the region between the SW group and the center of Coma, shows a very asymmetric gas distribution. Most of the HI gas is placed in the west side, while the east appears depleted. It has a high relative velocity to the main cluster ( $\sim 1500 \text{ km s}^{-1}$ ).
- **CGCG 160–076** This HI rich galaxy, with  $\text{Def}=-0.65$ , is placed at  $40'$  ( $0.8 \text{ Mpc}$ ) in the north of Coma. It was previously tentatively imaged in 21 cm by Sullivan (1989), who reported an offset between the optical and HI positions. We do not confirm this result.
- **CGCG 160–086** This blue disk galaxy is projected onto the SE edge of the X-ray emission. The detection of this galaxy is less reliable than the others because the data cube was contaminated by interference close to the position of the galaxy.
- **IC 4040** This blue disk galaxy is, among our detections, the closest to the cluster center. It is HI deficient ( $\text{Def}_{\text{HI}}=0.61$ ), and its neutral gas distribution is asymmetric, with most of the HI in the SE, while the NW appears depleted.
- **IC 842** This late type spiral is in the NE of Coma,  $\sim 1^\circ$  from the cluster center. Its HI distribution is regular and slightly larger than the optical disk. We obtained a rather normal HI content,  $\text{Def}_{\text{HI}}=0.31$ , compared with previous observations (see Sect. 3.1).
- **KUG 1258+287 & FOCA 195** These two galaxies, very close to each other, are detected for the first time in 21 cm. They are placed in the north, at  $\sim 36'$  ( $0.72 \text{ Mpc}$ ) from the cluster center. Our velocity estimation for FOCA 195 is the first ever reported. Regular gas distributions, and normal HI contents for both galaxies were found. We detected an independent HI emission, still to be confirmed,  $1.4'$  W of KUG 1258+287, with no optical counterpart seen in the DSS. We estimate a total HI mass of  $2.2 \times 10^8 M_\odot$  for this detection.
- **NGC 4907** This bright Sb spiral, projected at only  $19'$  ( $\sim 0.38 \text{ Mpc}$ ) NE of the Coma core, is another newly HI detected galaxy. The HI map shows a HI disk clearly smaller than the optical one, what is expected for such an HI deficient galaxy:  $\text{Def}_{\text{HI}}=0.99$ . It appears a striking feature extending through  $24''$  ( $\sim 8 \text{ kpc}$ ) to the NW of the galaxy, but as this emission appears in only one independent channel it should be confirmed by future observations.
- **NGC 4911** This is one of the two giant spirals in Coma, projected at  $20'$  ( $\sim 0.4 \text{ Mpc}$ ) SE of the core. It is HI deficient ( $\text{Def}_{\text{HI}}=0.58$ ), and presents an offset of 5–10 arcsec between HI and optical positions. A striking emission is detected SW of this galaxy (not shown in Fig. 2), what suggests a close interaction with its neighbour DRCG 27-62. We will discuss this result in a future paper.
- **NGC 4922/KPG 363–B** This interacting pair lies at the northern periphery of Coma. An absorption and an emission HI features are present, both



coinciding with the northern spiral galaxy. Gavazzi (1987) reported two emission features in both sides of the absorption line, but we detect the emission only in the lower velocity side ( $6892 \text{ km s}^{-1}$ ). This emission is seriously contaminated by the absorption, and we obtained a total flux of  $0.12 \text{ Jy km s}^{-1}$ , only half of the value reported by Gavazzi (1989).

- **CGCG 160–098** This is the HI richest galaxy among the blue disks reported by Bothun & Dressler (1986) in Coma. It is the only blue disk galaxy located outside the X–ray emission,  $50'$  NE from the cluster center. Its HI map extends well beyond the optical disk and it shows a normal HI content ( $\text{Def}_{\text{HI}}=0.16$ ).
- **NGC 4921** This is the other giant spiral in Coma, also projected close to the cluster center, at  $25'$  SE ( $\sim 0.5 \text{ Mpc}$ ). We obtain a very high HI deficiency:  $\text{Def}_{\text{HI}}=1.11$ . It shows a very perturbed gas distribution, which is clearly less extended than the optical disk. Most of the HI emission is distributed along the SE spiral arm, while the NW appears depleted. The HI centroid exhibits a slight offset,  $10''$  E of the optical center.
- **IC 4088** Observed in the far northern field, this galaxy shows a normal HI content ( $\text{Def}=-0.01$ ), and a regular HI distribution. Three dwarf systems, clearly detected in HI, encircle this galaxy; optical DSS counterparts are associated with the dwarfs.
- **NGC 4926–A** Blue disk galaxy projected near the SE edge of the X–ray source. It shows a normal HI content

( $\text{Def}=0.16$ ) and a similar extension for optical and HI disks. Our 21 cm velocity ( $V=6876 \text{ km s}^{-1}$ ) is significantly lower than the optical velocity reported ( $7100 \text{ km s}^{-1}$ , Amram et al. 1992).

## REFERENCES

- Amram, P., Le Coarer, E., Marcelin, M., Balkowski, C., Sullivan, W., & Cayatte, V. 1992, *A&AS*, 94, 175
- Barnes, J. E. 1998, in "Galaxies: interactions and induced star formation", Saas Fee Advanced Course 26, eds D. Friedli, L. Martinet and D. Pfenniger.
- Bekki, K. 1999, *ApJ*, 510, L15
- Biviano, A., Durret, F., Gerbal, D., Le Fèvre, O., Lobo, C., Mazure, A., & Slezak, E. 1996, *A&A*, 311, 95
- Biviano, A. 1998, private communication.
- Boselli, A., Gavazzi, G., Lequeux, J., Buat, V., Casoli, F., Dickey, J., & Donas, J. 1997, *A&A*, 327, 522
- Bothun, G., Aaronson, M., Schommer, R., Mould, J., Huchra, J. P., & Sullivan, W. 1985, *ApJS*, 57, 423
- Bothun, G., & Dressler, A. 1986, *ApJ.*, 301, 57
- Bravo-Alfaro, H. 1997, Ph. D. thesis, Université de Paris VII
- Bravo-Alfaro, H., Szomoru, A., Cayatte, V., Balkowski, C., & Sancisi, R. 1997, *A&AS*, 126, 537
- Bravo-Alfaro, Cayatte, V., van Gorkom, J. H., & Balkowski, C. 2000, in preparation.
- Briel, U. G., Henry, J. P., & Bohringer, H. 1992, *A&A*, 259, L31
- Burns, J. O., Roettiger, K., Ledlow, M., & Klypin, A. 1994, *ApJ*, 427, L87
- Butcher, H. R., & Oemler, A. 1978, *ApJ*, 219, 18
- Butcher, H. R., & Oemler, A. 1984, *ApJ*, 285, 426
- Caldwell, N., Rose, J. A., Sharpless, R. M., Ellis, R. S., & Bower, R. G. 1993, *AJ*, 106, 473
- Caldwell, N., & Rose, J. A. 1997, *AJ*, 113, 492
- Caldwell, N., Rose, J. A., & Dendy, K. 1999, *AJ*, 117, 140
- Casoli, F., Boissé, P., Combes, F., Dupraz, C. 1991, *A&A*, 249, 359
- Cayatte, V., van Gorkom, J. H., Balkowski, C., & Kotanyi, C. 1990, *AJ*, 100, 604
- Cayatte, V., Kotanyi, C., Balkowski, C., & van Gorkom, J. H. 1994, *AJ*, 107, 1003
- Chamaraux, P., Balkowski, C., & Gérard, E. 1980, *A&A*, 83, 38
- Chincarini, G., Giovanelli, R., & Haynes, M. P. 1983 *ApJ*, 269, 13
- Colless, M., & Dunn, A. M. 1996, *ApJ*, 458, 435
- Combes, F., Dupraz, C., Casoli, F., & Pagani, L. 1988, *A&A*, 203, L9
- Conselice, C. J., & Gallagher, J. S. III 1998, *MNRAS*, 297, L34
- Dickey, J. M. 1997, *AJ*, 113, 1939
- Donas, J., Buat, V., Milliard, B., & Laget, M. 1990, *A&A*, 235, 60
- Donas, J., Milliard, B., & Laget, M. 1995, *A&A*, 303, 661

- Donnelly, R. H., Markevitch, M., Forman, W., Jones, C., Churazov, E., & Gilfanov, M. 1999, *ApJ*, 513, 690
- Dressler, A. 1980, *ApJSS*, 42, 565
- Dressler, A., & Gunn, J. E. 1990, in *Evolution of the Universe of Galaxies: Edwin Hubble Centennial Symposium*. ed. R. Kron (San Francisco: Astronomical Society of the Pacific), p. 200
- Dressler, A., & Gunn, J. E. 1992, *ApJS*, 78, 1
- Dressler, A., Smail, I., Poggianti, B. M., Butcher, H., Couch, W. J., Ellis, R. S., & Oemler, A. 1999, *ApJS*, 122, 51
- Gavazzi, G. 1987, *ApJ*, 320, 96
- Gavazzi, G. 1989, *ApJ*, 346, 59
- Giovanelli, R., & Haynes, M. P. 1983, *AJ*, 88, 881
- Giovanelli, R., & Haynes, M. P. 1985, *ApJ*, 292, 404
- Girardi, M., Fadda, D., Giurcin, G., Mardirossian, F., Mezzetti, M., & Biviano, A. 1994, *ApJ*, 457, 61
- Haynes, M. P., & Giovanelli, R., Herter, T., Vogt, N. P., Freudling, W., Maia, M. A. G., Salzer, J. J., & Wegner, G. 1997, *AJ*, 113, 1197
- Huchra, J. P., Geller, M. J., de Lapparent, V., & Corwin, H. G. jr. 1990, *ApJSS*, 72, 433
- Kenney, J. D. P., & Young, J. S. 1989, *ApJ*, 344, 171
- Lavezzi, T. E., Dickey, J. M., Casoli, F., & Kazès, I. 1999, *ApJ*, 117, 1995
- McMahon, P. M. 1993, Ph.D. thesis, Columbia University, U.S.A.
- Mellier, Y., Soucail, G., Fort, B., & Mathez, G. 1988, *A&A*, 199, 67
- Mirabel, I. F., & Sanders, D. B. 1988, *ApJ*, 355, 104
- Moore, B., Katz, N., Lake, G., Dressler, A., & Oemler, A. 1996, *Nat*, 379, 613
- Moore, B., Lake, G., Quinn, T., & Stadel, J. 1999, *MNRAS*, 304, 465
- Oemler, A. 1992, in *Clusters and Superclusters of Galaxies*. ed. A. C. Fabian (Dordrecht:Kluwer), p. 29
- Poggianti, B. M., Smail, I., Dressler, A., Couch, W. J. Barger, A. J., Butcher, H., Ellis, R. S., & Oemler, A. 1999, *ApJ*, 518, 576
- Roettiger, K., Burns, J. O., & Loken, C. 1996, *ApJ*, 473, 651
- Stevens, I. R., Acreman, D. M., & Ponman, T. J. 1999, *MNRAS*, in press.
- Sullivan, W. 1989, in *The World of Galaxies*, ed. H. G. Corwin, Jr., & L. Bottinelli (New York: Springer), p. 404
- Thomas, P. A., Colberg, J. M., Couchman, H. M. P., Efstathiou, G. P., Frenk, C. S., Jenkins, A. R., Nelson, A. H., Hutchings, R. M., Peacock, J. A., Pearce, F. R., & White S. D. M. 1998, *MNRAS*, 296, 1061
- Valluri, M., van Gorkom, J. H., & McMahon, P. M. 1999, submitted to *AJ*
- van den Bergh, S. 1976, *ApJ*, 206, 883

van Gorkom, J. H., Balkowski, C., & Kotanyi, C. 1984, in *Clusters and Groups of Galaxies*, ed. F. Mardirossian, G. Giuricin, & M. Mezzetti (Dordrecht: Reidel), p. 261

van Gorkom, J. H. 1996, *The Evolution of Galaxies in Different Environments*, in the Minnesota Lectures on Extragalactic HI, ed. E. D. Skillman, ASP Conf. Series, 106, 293

Verheijen, M. A. W. 1996, in *Cold Gas at High Redshifts*, eds. M. Bremer, P. van der Werf, and C. L. Carilli. Kluwer: Dordrecht p. 165

Vikhlinin, A., Forman, W., & Jones, C. 1997, *ApJ*, 474, L7

Warmels, R. H. 1988, *A&AS*, 72, 19

White, S. D. M., Briel, U. G., & Henry, J. P. 1993, *MNRAS*, 261, L8

Wilson, M. A. G. 1970, *MNRAS*, 151, 1

Fig. A1.— Plot of the 12 observed fields in Coma. The size of the circles indicates the effective field of view of each pointing. The segmented circle outlines the 1 Abell radius of Coma (1.2 degrees). Crosses indicate detected galaxies and the asterisk indicates the cluster center, coincident with the giant galaxy NGC 4874.

Fig. A2.— Composite plot of individual HI maps of spiral galaxies of Coma observed with the VLA. Galaxies are shown at their proper position (except those in the rectangle, where the position of CGCG 160–102 is indicated with an “x”) and they are magnified by a factor of 7. The HI maps are overlaid on DSS optical images. The first contour is the same for all galaxies, corresponding to  $3 \times 10^{19}$  cm<sup>-2</sup>. Their identification and central velocities (in km s<sup>-1</sup>) are indicated. The large scale contours sketch the X-ray emission as observed by Vikhlinin et al. 1997. The cross indicates the cluster center, coincident with the elliptical NGC 4874.

Fig. A3.— Comparison of total HI flux obtained in this work with previous 21 cm observations. The dotted line indicates the 45° fit position. Solid lines join different estimations done for the same object. Reference keys are: Gavazzi 1987 (G87), Gavazzi 1989 (G89), Giovanelli and Haynes 1985 (GH85), Bothun et al. 1985 (B85), Chincarini et al. 1983 (C83), and Haynes et al. 1997 (H97)

Fig. A4.— The distribution of the HI deficiency parameter as a function of the projected radius from the center of Coma. Black circles correspond to detected galaxies, and triangles to lower limits for non detected.

Fig. A5.— The position of the detected (crosses) and non-detected (triangles) galax-

---

This 2-column preprint was prepared with the AAS L<sup>A</sup>T<sub>E</sub>X macros v4.0.

ies in the present survey, superposed on the ROSAT X-ray emission (Vikhlinin et al. 1997).

Fig. A6.— The position of the detected (crosses) and non-detected (triangles) starburst galaxies, as well as the non-detected (dotted points) PSBs. They are superposed on the ROSAT X-ray emission (Vikhlinin et al. 1997).

Fig. A7.— The plot mUV-b color versus the HI deficiency parameter. The linear fit is indicated. A clear correlation is seen in spite of the high dispersion (the correlation coefficient is 0.61).

Fig. A8.— The plot mUV-b color versus the molecular gas content, given by the ratio  $M_{H_2}/\text{optical disk area (pc}^2\text{)}$ . A weak correlation is found (correlation coefficient of 0.47).

Fig. A9.— Plot of mUV-b color versus the number of neighboring galaxies inside a  $5'$  radius (from NED). Blue galaxies do not have a larger number of close neighbours than red ones, making it unlikely that major galaxy-galaxy interactions have triggered the starburst.

TABLE 1  
OBSERVATIONAL PARAMETERS

(1) Field	(2) $\alpha_{1950}$ h m s	(3) $\delta_{1950}$ ° ' "	(4) Config VLA	(5) $t_{\text{int}}$ hrs	(6) Bandwidth MHz	(7) Central vel km s <sup>-1</sup>	(8) $\Delta v$ km s <sup>-1</sup>	(9) rms mJy/beam	(10) mJy-K conv mJy/beam
1	12 58 44.8	28 18 05.0	C	4.0	6.25	7800	21.5	0.40	1.29
			D	20.0	6.25	7650	21.5	0.20	5.47
2	12 58 30.0	28 18 00.0	C	4.0	6.25	5500	21.5	0.39	1.43
			D	2.0	6.25	5500	43.3	0.32	4.81
3	12 55 24.4	28 43 10.5	C	4.0	6.25	7300	21.5	0.42	1.32
4	12 59 05.0	28 00 00.0	C	4.0	6.25	7200	21.5	0.40	1.42
			D	2.0	6.25	7200	43.3	0.35	4.85
5	12 59 00.0	29 23 58.0	C	4.0	6.25	7000	21.5	0.38	1.42
			D	2.0	6.25	7000	43.3	0.29	4.84
6	12 59 00.8	28 47 28.0	C	4.0	6.25	8600	21.5	0.42	1.26
7	12 56 40.4	27 54 55.0	C	4.0	6.25	5500	21.5	0.38	1.33
8	12 54 59.2	27 38 09.0	C	4.0	6.25	7300	21.5	0.40	1.31
9	12 57 31.5	28 18 24.0	C	4.0	6.25	9600	21.5	0.40	1.29
10	12 55 38.4	28 05 20.0	C	4.0	6.25	7300	21.5	0.40	1.32
			D	15.0	6.25	7300	21.5	0.20	5.46
11	13 01 26.0	28 27 14.0	C	4.0	6.25	7000	21.5	0.37	1.31
12	12 57 15.4	28 54 12.0	C	4.0	6.25	5400	21.5	0.40	1.28

TABLE 2  
GALAXIES DETECTED IN HI.

(1) CGCG	(2) Other name	(3) $\alpha_{1950}$ h m s	(4) $\delta_{1950}$ ° ' "	(5) Config	(6) Beam "	(7) Morph Type	(8) $B_T$	(9) $m_{UV-b}$
(1) 160-026	IC 3913	12 54 03.0	27 33 40.7	C	30.7×27.2	Sc <sup>1</sup>	15.4	-0.46
(2) 160-055	NGC 4848	12 55 40.7	28 30 45.0	C	30.5×27.5	Scd	14.4	-0.70
(3) 160-058		12 55 44.7	28 58 40.9	C	30.5×27.5	Sc	15.5	0.27
(4)	KUG 1255+275	12 55 53.4	27 34 49.1	C	30.7×27.2	Irr	16.3	-0.92
(5) 160-067	Mrk 057	12 56 12.0	27 26 44.4	C	30.7×27.2	Sa <sup>1</sup>	15.1	-0.90
(6) 160-073	Mrk 058	12 56 40.4	27 54 48.9	C	30.3×27.6	Sb	15.2	-0.30
(7) 160-076		12 57 15.7	28 54 01.3	C	29.9×26.9	Sbc	15.7	-1.35
(8) 160-086		12 58 08.9	27 54 24.8	C+D	35.2×33.0	Sb	15.6	-0.94
(9) 160-252	IC 4040	12 58 13.3	28 19 35.0	C+D	40.7×38.0	Sdm	15.4	-0.59
(10) 160-088	IC 842	12 58 15.5	29 17 18.5	C+D	36.6×35.4	Sc <sup>1</sup>	14.7	
(11)	KUG 1258+287	12 58 16.2	28 47 20.0	C	30.2×26.7	S*	16.4	-1.11
(12) 160-257	NGC 4907	12 58 24.3	28 25 38.3	C+D	39.8×34.5	Sb	14.5	0.70
(13) 160-260	NGC 4911	12 58 31.5	28 03 34.1	C+D	40.7×38.0	Sb	13.6	0.75
(14)	FOCA 195	12 58 50.7	28 47 26.2	C	30.2×26.7		17.3 <sup>1</sup>	-1.47
(15) 160-096	NGC 4922/	12 59 00.2 <sup>1</sup>	29 34 36 <sup>1</sup>	C+D	36.6×35.4	S0 <sup>1</sup>	13.9	
	KPG 363-B	12 59 01.4 <sup>1</sup>	29 34 58 <sup>1</sup>	C+D	36.6×35.4	Sb <sup>2</sup>	14.8	
(16) 160-098		12 59 00.8	28 56 45.5	C	30.2×26.7	Sbc	15.3	-0.13
(17) 160-095	NGC 4921	12 59 01.6	28 09 17.2	C+D	39.8×34.5	Sb	13.3	1.35
(18) 160-102	IC 4088	12 59 19.3	29 18 47.2	C+D	36.6×35.4	Sb <sup>1</sup>	14.7	
(19) 160-106	NGC 4926-A	12 59 43.3	27 55 00.7	C+D	35.2×33.0	Sa	15.4	0.21

TABLE 3  
HI PARAMETERS

(1) CGCG	(2) Other name	(3) Field	(4) $v_c$ km s <sup>-1</sup>	(5) $\Delta v$ km s <sup>-1</sup>	(6) HI flux Jy km s <sup>-1</sup>	(7) $F_{\text{cont}}$ mJy	(8) $M_{\text{HI}}$ 10 <sup>9</sup> M <sub>⊙</sub>	(9) Def <sub>HI</sub>	(10) r/r <sub>A</sub>
(1) 160-026	IC 3913	8	7538	260	1.08±0.06	1.73	1.25	0.04	0.80
(2) 160-055	NGC 4848	3	7041	130	0.37±0.03	16.56	0.43	1.14	0.36
(3) 160-058		3	7614	281	1.67±0.06	4.71	1.93	0.12	0.68
(4)	KUG 1255+275	8	7398	281	0.65±0.05	2.02	0.75	-0.17	0.59
(5) 160-067	Mrk 057	8	7657	194	1.07±0.04	3.34	1.24	-0.44	0.68
(6) 160-073	Mrk 058	7	5425	64	0.17±0.02	5.46	0.20	0.51	0.28
(7) 160-076		12	5390	235	2.00±0.06	5.20	2.31	-0.65	0.55
(8) 160-086		4	7481	130	0.15±0.02	3.76	0.17	0.58	0.33
(9) 160-252	IC 4040	1	7758	347	0.29±0.06	15.0	0.33	0.61	0.20
(10) 160-088	IC 842	5	7281	389	1.50±0.04	2.67	1.73	0.31	0.90
(11)	KUG 1258+287	6	8884	306	1.17±0.06	7.12	1.35	0.01	0.51
(12) 160-257	NGC 4907	2	5821	214	0.21±0.03		0.24	0.99	0.27
(13) 160-260	NGC 4911	1	7997	348	0.80±0.07	11.92	0.93	0.58	0.28
(14)	FOCA 195	6	8426	218	0.57±0.04		0.66	-0.11	0.55
(15) 160-096	NGC 4922/ KPG 363-B	5 5	6892 7086	130	0.12±0.02	27.47 27.47	0.14	1.28	1.17
(16) 160-098		6	8764	153	0.63±0.04	5.67	0.73	0.16	0.69
(17) 160-095	NGC 4921	2	5479	214	0.61±0.03	4.87	0.70	1.11	0.34
(18) 160-102	IC 4088	5	7108	475	3.46±0.07	8.50	4.00	-0.01	0.98
(19) 160-106	NGC 4926-A	4	6876	216	0.52±0.03	3.09	0.60	0.16	0.52

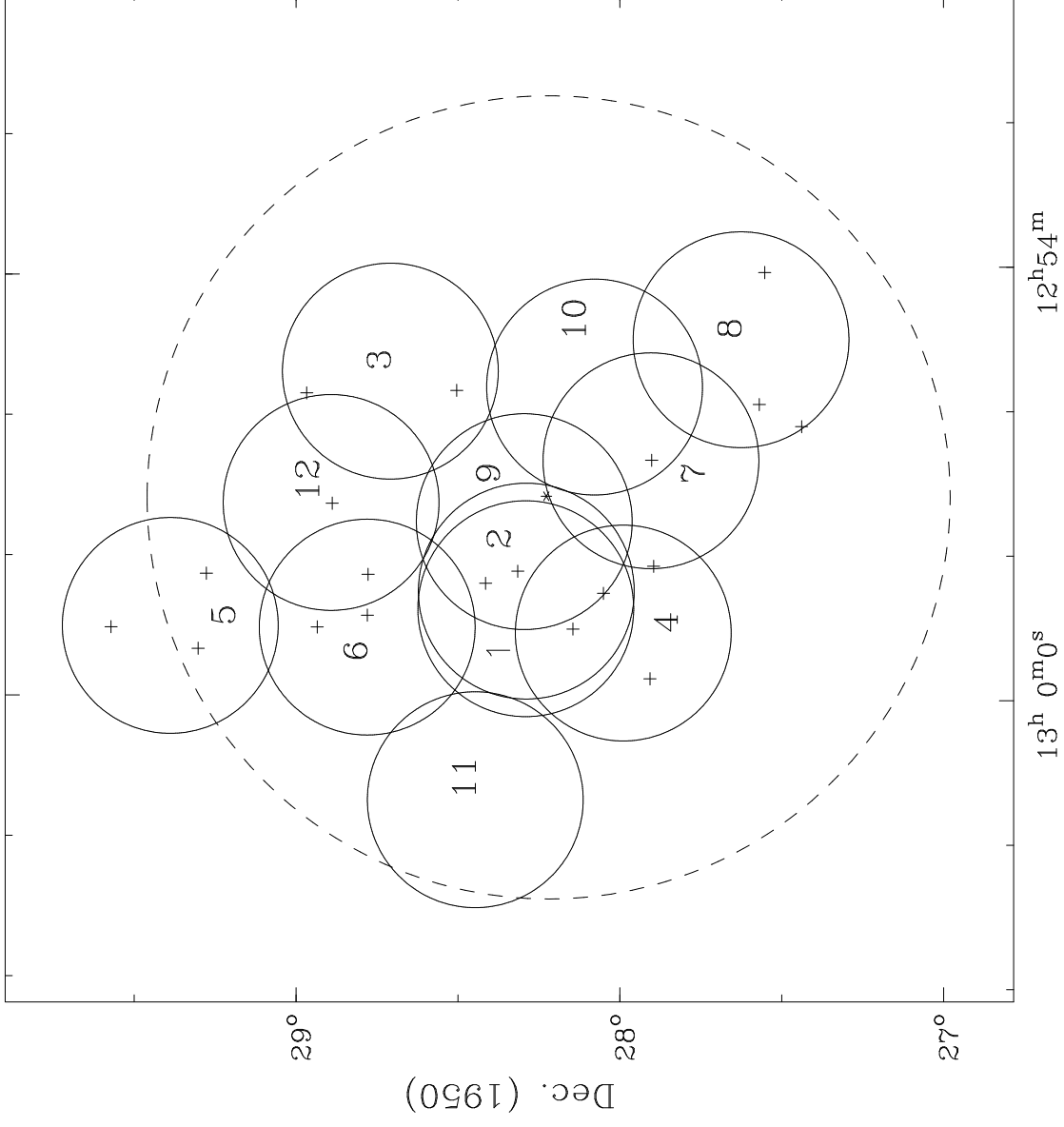


TABLE 4  
GALAXIES NON-DETECTED IN HI

(1) Name	(2) Other name	(3) $\alpha_{1950}$ h m s	(4) $\delta_{1950}$ ° ' "	(5) field	(6) Morph type	(7) $v_{\text{hel}}$ km s <sup>-1</sup>	(8) rms mJy/beam	(9) $M_{\text{HI}}$ 10 <sup>8</sup> M <sub>⊙</sub>	(10) Def <sub>HI</sub>
160-031	MCG 5-31-19	12 54 24.1	27 21 50	8	Sa <sup>2</sup>	6849	0.80	<1.2	>1.07
160-043	UGC 8071	12 55 04.0	28 27 40	3	Sa	7069	0.78	<1.2	>1.22
160-061	NGC 4851	12 55 56.8	28 25 06	10	SBa	7781	0.35	<0.5	>1.14
160-064	Mrk 056	12 56 09.4	27 32 10	8	Sa*	7392	0.76	<1.1	>0.69
160-069	IC 3943	12 56 11.5	28 22 59	10	S0/a	6704	0.31	<0.5	>1.32
160-213	NGC 4858	12 56 36.9	28 23 14	9	Sc (SB)	9456	0.62	<0.9	>0.93
160-216	IC 3955	12 56 41.0	28 15 59	10	SB0/a	7650	0.22	<0.3	>1.01
	KG1258+277	12 58 04.0	27 47 06	4	S0*	7651	0.62	<0.9	>0.70
160-261		12 58 35.0	28 10 13	4	S0/a	6866	0.40	<0.6	>1.27
160-108	MCG 5-31-108	12 59 48.1	28 29 07	1	Sb	8309	0.80	<1.2	>0.73
160-112	IC 4106	13 00 14.6	28 23 05	11	S0/a	7443	0.68	<1.0	>1.14
160-124	NGC 4944	13 01 26.0	28 27 14	11	S0/a <sup>3</sup>	7034	0.37	<0.6	>1.90

TABLE 5  
SB AND PSB GALAXIES NON-DETECTED IN HI

(1) ID	(2) Other name	(3) field	(4) $\alpha_{1950}$ h m s	(5) $\delta_{1950}$ ° ' "	(6) Morph type	(7) $v_{\text{hel}}$ km s <sup>-1</sup>	(8) rms mJy/beam	(9) $M_{\text{HI}}$ 10 <sup>8</sup> M <sub>⊙</sub>
D 77	Leda 83676	10	12 54 39.2	28 02 35	S0/a (SB)	7544	0.39	<0.6
D 94	Leda 83682	10	12 54 52.6	28 04 51	SA0 (PSB)	7084	0.35	<0.5
D 112	Leda 83684	10	12 54 56.4	28 09 02	SB0 (PSB)	7428	0.27	<0.4
D 21	MCG 5-31-037	8	12 55 36.3	27 45 33	SBa (PSB)	7684	0.48	<0.7
D 73	RB 183	7	12 55 53.9	28 01 54	SA0 (PSB)	5434	0.61	<0.9
D 44	KUG1256+278A	10	12 56 03.1	27 49 45	S0 (SB)	7554	0.37	<0.6
D 43	NGC 4853	10	12 56 10.1	27 51 58	SA0 (SB)	7660	0.32	<0.5
D 89	IC 3949	10	12 56 31.4	28 06 12.1	SA0 (PSB)	7378	0.18	<0.3
D 127	RB 042	10	12 57 15.4	28 14 16	S0 (PSB)	7514	0.41	<0.6
D 216	RB 160	1	12 57 38.2	28 30 34	Sa (PSB)	7684	0.46	<0.7
D 99	Mrk 060	9	12 57 45.4	28 07 59	SB0 (PSB)	9902	0.48	<0.7
D 146	RB 110	1	12 58 14.1	28 17 00	S0 (PSB)	7537	0.20	<0.3
D 61	CGCG 160-104	4	12 59 35.6	28 03 04	SA0 (PSB)	7102	0.44	<0.7
D 189	Leda 83763	2	12 59 49.9	28 22 13	S0 (PSB)	5937	0.97	<1.5



R.A. (1950)

